Surface effects in nucleation and growth of smectic-*B* crystals in thin samples

T. Börzsönyi[1,2] and S. Akamatsu[1,*]

[1]*Groupe de Physique des Solides, CNRS UMR 7588, Universités Denis-Diderot et Pierre-et-Marie-Curie, Tour 23, 2 place Jussieu, 75251 Paris Cedex 05, France*

[2]*Research Institute for Solid State Physics and Optics, Hungarian Academy of Sciences, P.O. BOX 49, H-1525 Budapest, Hungary*

(Received 29 July 2002; published 19 November 2002)

We present an experimental study of the surface effects (interactions with the container walls) during the nucleation and growth of smectic-*B* (SmB) crystals from the nematic in free growth and directional solidification of a mesogenic molecule [C_4H_9-(C_6H_{10})$_2$CN] called CCH4 in thin (of thickness in the 10-μm range) samples. We follow the dynamics of the system in real time with a polarizing microscope. The inner surfaces of the glass-plate samples are coated with polymeric films, either rubbed polyimid (PI) films or mono-oriented poly(tetrafluoroethylene) (PTFE) films deposited by friction at high temperature. The orientation of the nematic and the smectic-*B* is planar. In PI-coated samples, the orientation effect of SmB crystals is mediated by the nematic, whereas, in PTFE-coated samples, it results from a homoepitaxy phenomenon occurring for two degenerate orientations. A recrystallization phenomenon partly destroys the initial distribution of crystal orientations. In directional solidification of polycrystals in PTFE-coated samples, a particular dynamics of faceted grain boundary grooves is at the origin of a dynamical mechanism of grain selection. Surface effects also are responsible for the nucleation of misoriented terraces on facets and the generation of lattice defects in the solid.

DOI: 10.1103/PhysRevE.66.051709 PACS number(s): 64.70.Md, 81.10.Aj, 64.70.Dv, 68.70.+w

I. INTRODUCTION

The appearance of molecular crystals in a supercooled liquid occurs generally by a heterogeneous-nucleation process. In many cases, the walls of the container play the role of preferential nucleation substrate. Depending on the nature of that substrate, crystals may grow in epitaxy with it, and their orientation be well controlled. It has been known for a long time that one can also orient mesophases in thin (of thickness in the 10-μm range) samples of a mesogenic molecule by coating the inner surfaces of the container, generally made of glass, with a molecularly thin film of suitable nature and topography [1]. For nematic and smectic-*A* phases, the microscopic mechanism of phase orientation at play is a combination of surface energy minimization and elastic effects specific of the short-range orientational order proper to those phases [2]. Recently, surface coatings promoting both the alignment of a mesophase and the selection of the orientation of a smectic-*B* (SmB) phase in coexistence with it have been used in free growth (solidification in a uniformly undercooled sample) [3–7] and directional solidification (solidification at a constant speed V along a fixed temperature gradient G) [8–10] of different mesogenic molecules in thin samples (Fig. 1). A SmB phase is a true crystal with long-range positional order in the three directions of space—it is not a mesophase, but a lamellar plastic crystal. Thanks to the possibility of controlling the orientation of the two coexisting phases, a variety of new stationary, faceted growth patterns, resulting from a complex combination of a diffusion controlled dynamics and of a nonlinear growth kinetics proper to facet orientations, has been discovered [10]. However, some effects of the interactions between the molecules and the walls of the container (surface effects) on the growth dynamics of the crystal remain to be studied.

In this paper, we present an experimental study of surface effects during the nucleation and growth of SmB crystals from the nematic phase of the mesogenic molecule C_4H_9-(C_6H_{10})$_2$CN (in short, CCH4). The inner surfaces of our glass-wall samples are coated with molecularly thin polymer films, either rubbed polyimid (PI) films [1,11] or mono-oriented poly(tetrafluoroethylene) (PTFE) films deposited by friction transfer at high temperature [12–16]. The CCH4 substance is a member of a series of mesogenic molecules, noted CCHm, where $m=3$ to 5 is the length of the aliphatic chain of the amphiphilic liquid crystal, which undergoes a first-order transition from the nematic to the SmB phase at a temperature T_{NS} which depends slightly on m ($T_{NS}\approx 53$°C for CCH4) [17]. We used both the thin-sample free growth (TFG) and thin-sample directional solidification (TDS) methods to observe the time evolution of the shape of

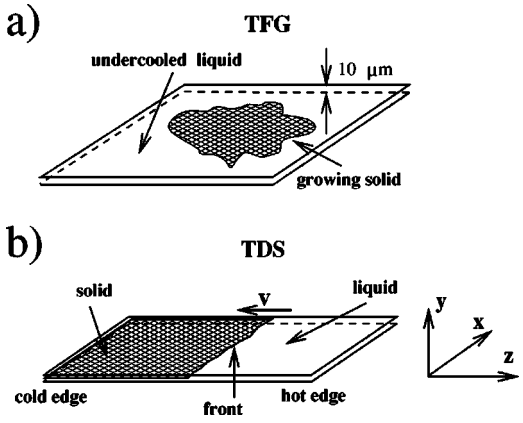

FIG. 1. Principle of thin-sample solidification experiments: (a) TFG, thin-sample free growth; (b) TDS, thin-sample directional solidification. z axis of the thermal gradient G. x axis parallel to the isotherms. y, transverse direction. V, pulling velocity.

*Electronic address: akamatsu@gps.jussieu.fr

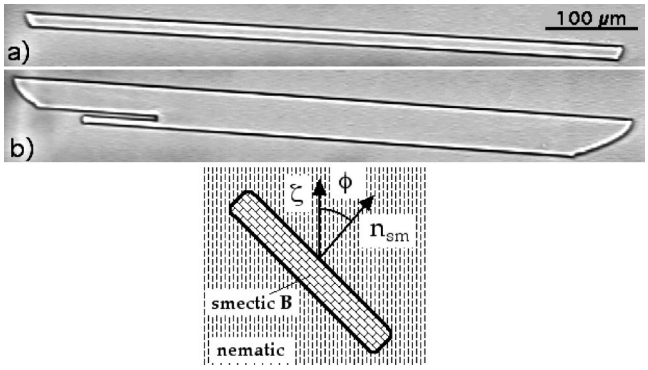

FIG. 2. Thin-sample free growth of a smectic-*B* crystal of CCH4 in a 10-μm thick PI-coated sample (the rubbing axis ζ is vertical). No polars. (a) $\Delta T = 0.07$ K. The facets do not grow. (b) $\Delta T = 0.11$ K. The facets grow, and the tips undergo a morphological instability. Bottom: definition of the disorientation angle ϕ and the vector normal to the smectic layers $\mathbf{n}_{sm}$.

the solid-liquid interface with an optical microscope. The practically two-dimensional (2D) character of the samples implies that the solid-liquid interface remains essentially perpendicular to the sample plane. In the situations considered in the present study, there is no convection in the liquid, and matter exchanges occur only by diffusion.

Near equilibrium, SmB crystals in coexistence with the nematic exhibit a single facet plane, namely, the smectic-layer plane (Fig. 2) [3]. The nematic-SmB interface is otherwise rough on a molecular scale. In PI- and PTFE-coated samples, a planar orientation (see below) is imposed not only to the nematic, but also to the SmB phase. In freshly filled samples, i.e., CCH4 nematic samples in which no crystallization has yet occurred, the nematic is aligned along the direction ζ of rubbing (for PI) or friction (for PTFE) of the polymer film. For a planar orientation of the SmB phase, the smectic layers, thus the facets of the nematic-SmB interface, are perpendicular to the sample plane, so that the 2D character of the system is guaranteed. The partly faceted crystals then grow in a well-oriented nematic that presents large regions free of defects, which, if present, would perturb the interface.

Most previous experimental studies of the growth dynamics of CCH*m* SmB crystals were performed in TFG in PI-coated samples [3–7]. In a more recent TDS study, thin CCH4 PTFE-coated samples were used for the first time [10], in order to increase the strength of the selection of the in-plane orientation of SmB crystals. The purpose of the present paper is to cast light to the mechanisms at play in that selection. Therefore, we will focus our attention on the formation by heterogeneous nucleation and growth, and the coarsening of SmB polycrystals of CCH4 in TFG, and on the growth dynamics of such polycrystals in TDS. We reproduced some TFG experiments in PI-coated samples. We thus observed some unexpected phenomena, such as the rotation of highly misoriented crystals (see below) during the first stages of their growth. However, the most interesting results have been obtained in PTFE-coated samples, for reasons which will become clearer later on.

Our main TFG results can be summed up as follows. In

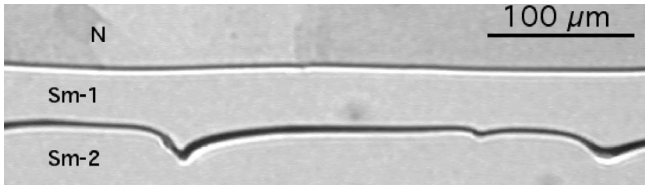

FIG. 3. Planar-front regime in thin-sample directional solidification of CCH4 in a PTFE-coated sample ($G = 54$ K cm^{-1}; $V = 0.9$ μm s^{-1}). The friction axis is vertical. In this, and all the following micrographs, growth is upwards. N, nematic. Sm-1, smectic-*B*. Sm-2, smectic-*B* oriented differently from Sm-1. Note the domains in the nematic. Sm-1 is a single crystal, but Sm-2 a polycrystal, as shown by the presence of cusps caused by grain boundaries on the interface between Sm-1 and Sm-2 (recrystallization front).

both PI- and PTFE-coated samples, many CCH4 SmB crystals of a planar orientation nucleate for undercoolings of a few 0.1 K. Let us define the (in-plane) disorientation angle ϕ as the angle between ζ and the unit vector $\mathbf{n}_{\mathrm{Sm}}$ normal to the smectic layers (Fig. 2). The average value of ϕ is equal to 0 in a PI-coated sample, but the width of its distribution about 0 is large ($\approx 60°$). This weak orientation selection effect and the above-mentioned process of rotation of highly misoriented crystals (i.e., of large ϕ values) suggest that the final in-plane orientation of SmB crystals in PI-coated samples is determined by the interactions of the crystals with the nematic. In contrast, in PTFE-coated samples, SmB crystals directly nucleate with either of two symmetrical disorientations $\pm\phi_{\mathrm{PTFE}}$ (about $\pm 13°$). This apparent epitaxial growth suggests the existence of a specific, strongly anisotropic interaction between the CCH4 molecules and the PTFE film on a molecular scale. This is supported by the existence of a strong ''memory effect'' [18,19] in remelted PTFE-coated samples. Such an effect is almost absent in PI-coated ones.

In TDS of single crystals of CCH4 [10], the front is generally (i.e., except for very special orientations) nonfaceted, and exhibits a dynamics similar to that of any nonfaceted crystal at small solidification rates. The front remains planar below a threshold velocity V_c (Fig. 3) and becomes cellular above V_c. Facets appear only above V_c, which causes the formation of localized objects, comparable to solitary waves, called ''facetons.'' In the case of polycrystal samples, that we consider in the present study, facets appear even for $V < V_c$ in the vicinity of grain boundaries (GBs). This has many consequences in PTFE-coated samples, the most remarkable of which is the existence of a mechanism of grain selection, the main ingredient of which are the particular dynamics of faceted grooves attached to GBs and the nucleation of SmB crystals ahead of the front. We study that mechanism in detail. We also consider the existence of a recrystallization front visible in the rear of the solidification front. Finally, a careful analysis of the stepwise growth dynamics of the facets allows us to identify a mechanism of generation of planar lattice defects in the solid.

II. EXPERIMENTAL SECTION

A. Preparation of the samples

The basic thermodynamical parameters of CCH4 (Merck) and the other CCH*m* compounds can be found in Refs.

[3,10]. The crystal parameters of the SmB phase of CCH4 were measured by small-angle x-ray scattering in a previous study [10] (see Ref. [17] for those of CCH3 and CCH5). The lamellar stacking of the molecules in the SmB is of the *AB* type for all CCH*m* compounds. The packing of the molecules within the layers is hexagonal. The phenomena of selection of crystal orientation in PI- and PTFE-coated samples do not depend qualitatively upon whether CCH3, CCH4, or CCH5 are considered. Some quantitative differences will be mentioned later on. As received, CCH4 contains a small amount of unknown impurities. A rough characterization of the residual impurities can be found in Ref. [10]—the thermal gap ΔT_0 is about 0.2 K, the partition coefficient 0.12, and the diffusion coefficient in the nematic 8×10^{-7} cm^2 s^{-1}. Because of a chemical decomposition taking place in the nematic phase, the impurity concentration in a given sample increases slowly in time, which shows up by a progressive decrease of the nematic-SmB equilibrium temperature T_{NS} (T_{NS} actually is the temperature of the liquidus of the alloy CCH4 + residual impurities). This is, however, of secondary importance for the present purpose.

The PI-coated cells (thickness $d = 10$ μm; lateral dimensions of 12×20 mm^2) were purchased from E.H.C Co., Japan. The PTFE-coated cells ($d = 12$ μm; lateral dimensions of 9×60 mm^2) were made in our laboratory. Mono-oriented PTFE films are deposited by slowly sliding a PTFE block pressed against the surface of a clean glass microslide maintained at a temperature slightly higher than 250 °C, along a direction ζ. No further treatment is applied. Two PTFE-coated plates, separated from each other by two parallel 12-μm thick plastic spacers, are assembled and glued so as to make a thin cell.

We filled our samples by capillarity, according to either of two different procedures. A first method (method 1), used in TFG only, consists of filling the sample *in situ* at a temperature higher than the isotropic-nematic equilibrium temperature T_{IN} (about 80 °C). The sample is then used without being sealed or outgased. In the second method (method 2), a sample is filled under an Ar atmosphere at a temperature higher than T_{NS}, then rapidly cooled down to room temperature, and sealed. It is then a SmB polycrystal, as a result of the heterogeneous nucleation of many crystals in the nematic.

B. Nematic alignment

When a nematic phase is in contact with a flat homogeneous wall, the orientation of the director **d** is an intermediate between two particular configurations, or anchorings, called ''homeotropic'' and ''planar,'' corresponding to **d** being perpendicular and parallel to the wall, respectively [2]. The surface induced order propagates over a macroscopic distance (persistence length) of order 1 μm into the bulk because of the particular elastic properties of the nematic. This allows one to obtain a uniformly aligned nematic when the sample is sufficiently thin. That a uniform planar (or almost planar [20]) alignment along a predefined direction ζ is obtained thanks to a gentle rubbing of a PI film with a soft textile brush is a well-known empirical fact. The physical origin (influence of a one-dimensional microscopic roughness, anisotropic and/or specific molecular interactions) of that effect still remains controversial [2,11,21].

Mono-oriented PTFE films have been known for a long time, at least empirically, to promote epitaxial growth of molecular crystals of various organic compounds [12–16]. Recently, their structure has been revealed by electron diffraction [15]; they are almost fully crystalline (as bulk PTFE is), whereas PI films are generally partly crystalline. A lattice matching between PTFE films and molecular crystals has been evidenced experimentally in a few cases [13]. On the other hand, atomic-force microscopy studies revealed that a mono-oriented PTFE film deposited at a temperature above 250 °C (as in the present study) onto a flat silicon wafer under well controlled conditions of temperature, pressure, and sliding speed, is not of uniform thickness, but always contains thin stripes of a typical thickness of 10 nm and a width of several 100 nm, lying parallel to the friction axis ζ [14,16]. These stripes, which are probably made of well-crystallized bunches of PTFE chains, remain perfectly rectilinear and uninterrupted along millimetric distances. This uniaxial roughness probably plays a major role in the alignment of the nematic along ζ [22].

In PI-coated samples, the alignment of the nematic along the rubbing axis is generally uniform, independently of the filling method (see below). In PTFE-coated samples filled according to method 1, and cooled down to a temperature slightly above T_{NS}, nematic regions with the expected average alignment along ζ delimited by more or less extended defect zones are observed. In the well-aligned regions, a faintly contrasted striation parallel to ζ is visible between crossed polars (see, for instance, Fig. 10 below). The defects between the aligned regions are clearly associated with imperfections of the PTFE film (small aggregates of the PTFE chains). The striation within the relatively uniform regions are probably due to exceptionally thick, but well-crystallized bunches of polymer chains. When prepared by method 2, PTFE-coated samples are always structured, in the nematic phase, into domains of different orientations. This phenomenon will be addressed in Sec. IV.

C. The TFG and TDS methods

Free-growth experiments [Fig. 1(a)] were performed in an Instec hot stage. The thermal stability of the setup is of a few mK. We chose a relatively slow cooling rate (about 0.01 K s^{-1}) in order to prevent the system to overshoot the desired value of the undercooling $\Delta T = T_{NS} - T$, where T is the targeted temperature. The SmB phase appears by heterogeneous nucleation, at a rate which depends on ΔT. No nucleation events are observed within several tenths of minutes for $\Delta T < 0.1$ K. Nucleation rarely occurred for ΔT between 0.1 and about 0.3 K in PI-coated samples. Within that ΔT range, the number of crystals appearing in the field of view of our optical setup (625×480 μm^2) does not exceed two in PTFE-coated samples. For the values of ΔT that we used generally (0.3–0.6 K), two to six crystals nucleate within a few seconds in an area of 10^{-1} mm^2. Unfortunately, nucleation occurs during the thermal transient of the

hot stage, so that the uncertainty on the value of ΔT is relatively large (0.05 K), which prevented us to perform a systematic study of the nucleation rate as a function of ΔT [23].

A detailed description of our TDS setup [Fig. 1(b)] can be found in Ref. [24]. We used values of V ranging from 1 to 30 μm s^{-1}. The value of G (from 30 to 80 K cm^{-1}) remained constant within less than 10% during a given solidification run. We used both PI- and PTFE-coated samples in TDS experiments, but most of the results shown here concern PTFE-coated samples. A typical TDS experiment is performed as follows. A thin sample of CCH4 is introduced in the solidification setup. It then melts partly. The nonmelted part of the sample is a polycrystal, but a large single crystal can be grown from it using funnel-shaped samples [10,24]. After a certain time (about 30 min) of maintain at rest ($V=0$) in order to homogenize the liquid, the solidification is started at a given velocity. A stationary regime is generally reached after a transient regime. Then, we apply one or several velocity changes and observe the response of the system to these changes.

Free growth and directional solidification were observed under the eye-piece of an optical microscope (Leica), either in the bright-field mode, or using rotating polars. Images were detected via a CCD camera coupled to a digital image processing device. Between crossed polars, a well-aligned planar nematic appears dark when, and only when, one of the two polars is parallel to the average direction of the director. As the optical axis of the SmB phase is normal to the smectic layers, a homeotropic SmB crystal appears always dark between crossed polars. On the other hand, the contrast between a planarly oriented SmB crystal and the surrounding planar nematic (or between two SmB grains of different orientations) depends on the disorientation angle ϕ. In principle, this yields a method for measuring ϕ for each grain of a polycrystal. In fact, because of the recrystallization process which destroys the initial SmB grain distribution (see below), such measurements had to be performed during growth.

III. GROWTH DYNAMICS OF CCH4 SMECTIC-*B* CRYSTALS

A. Free growth

In Secs. III A and III B, we summarize some TFG and TDS results obtained in previous studies. Though, in the present study, we will consider only planarly oriented crystals, it is useful to recall first that it is possible, with a suitable surface coating, to obtain thin samples of CCH*m* with a homeotropic orientation of the nematic and the SmB crystals. The smectic layers are then parallel to the sample plane. Homeotropic crystals of CCH*m* grow nonfaceted, thus according to a fully diffusion controlled dynamics, and 2D dendritic patterns are observed [7], which exhibit a sixfold symmetry. This is consistent with the hexagonal packing of the molecules within the smectic layers, and typical of a system with a small value of the interfacial anisotropy. If the homeotropic SmB crystal is surrounded by a planar nematic, this introduces an additional (twofold) term in the anisotropy (including that of the diffusion coefficient) which modifies the selection of the dendritic pattern.

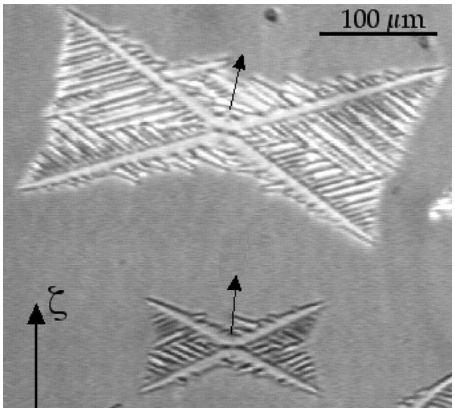

FIG. 4. Two SmB crystals of CCH4 growing in TFG in a 10-μm thick PI-coated sample ($\Delta T=0.4$ K). ζ, rubbing axis of the PI film. The snapshot was taken between polars. Note that no defects in the nematic alignment are visible. Small arrows, vector $\mathbf{n}_{\mathrm{Sm}}$ normal to the smectic layers for each crystal (see text).

Returning to planarly oriented crystals, we note that their orientation is fully specified by two angles, namely, the disorientation angle ϕ defined above (Fig. 2) and an angle α specifying the orientation of the hexagonal lattice with respect to the normal **y** to the sample plane. As the dependence of the interfacial properties on α is very weak—as proven by the observations performed in homeotropic samples—the dynamics of the nematic-SmB front for planarly oriented crystals does not depend sensitively on the angle α, and we will generally ignore it.

A planarly oriented SmB crystal maintained near equilibrium (or growing at low undercooling) exhibits an elongated shape, with two long facets perpendicular to the sample plane, and rounded ends. At low undercooling (less than about 0.1 K), the facets do not grow (''blocked'' facet), within experimental resolution, whereas the rounded ends progress with a growth rate less than 10 μm s^{-1} [Fig. 2(a)] [10]. For values of ΔT slightly higher than 0.1 K, the facets grow more or less smoothly. The existence of a threshold value of ΔT below which the facets do not grow signals that there is no active lattice defect (dislocations) intersecting the interface [25]. Thus the growth of the facets for $\Delta T>0.1$ K must involve a mechanism of nucleation of molecular terraces. A planarly oriented crystal growing at an undercooling larger than 0.1 K systematically undergoes shape instabilities due to impurity diffusion. For ΔT values between 0.1 and 0.3 K, a mere splitting of the tip [Fig. 2(b)] occurs. For $\Delta T>0.3$ K, dendriticlike patterns are observed (Fig. 4).

In the plane of the sample, the surface tension γ_{NS} of the nematic-SmB interface is highly anisotropic. The facet orientation corresponds to a singularity of the Wulff plot, i.e., the angular dependence of the surface tension $\gamma_{NS}(\mathbf{n})$ ($\mathbf{n}$ is the normal to the nematic-SmB interface) of the nematic-SmB interface, when $\mathbf{n}$ is parallel to the normal $\mathbf{n}_{\mathrm{Sm}}$ to the smectic layers. We did not notice any sign of the existence of forbidden orientations in the equilibrium shape. As concerns the interfacial kinetics, it is well represented by an aniso-

tropic linear kinetic coefficient $\beta(\mathbf{n})$ defined by $v_n = \beta(\mathbf{n})\Delta T_k$, where v_n is the (local) normal velocity of the interface and ΔT_k is the kinetic undercooling, for all orientations except in the close vicinity of $\mathbf{n}_{\mathrm{Sm}}$. Realistic $\gamma_{NS}(\mathbf{n})$ and $\beta(\mathbf{n})$ functions have been built previously, which account for the main features of the growth phenomena observed in CCH4 [6,10]. However, the respective contributions of the anisotropies of the surface tension and of the kinetic coefficient to the selection of the observed growth shapes are not known with precision. We also note that, if $\phi \neq 0$, the nematic is distorted over a distance comparable to the persistence length in a region surrounding the crystal, since different anchoring orientations are imposed along the SmB-nematic interface and along the glass plates. The elastic energy associated to that distortion increases obviously with the disorientation of the crystal. This may play some role in nucleation and growth phenomena, as we will see later on.

When the growing crystals exhibit large facets, the disorientation angle ϕ can be measured directly from the micrographs (Fig. 2). When the facets are hidden by the development of a dendritic pattern, ϕ can also be estimated (within 1° or 2°), since $\mathbf{n}_{\mathrm{Sm}}$ is parallel to the line bisecting the largest angle between two main dendritic arms (Fig. 4). This was checked by melting partly a dendritic crystal and letting it coarsen at a constant temperature until it reaches a faceted shape.

B. Directional solidification

The TDS method has been used extensively for the study of nonfaceted growth [24,26–31], but rarely for that of faceted growth. In general, faceted crystals exhibit many facets, the growth of which occurs far from equilibrium and is very sensitive to the structure of the interface on a molecular scale and to lattice defects [25]. As a consequence, their (nonlocal) growth dynamics is nonstationary on a macroscopic scale [32,33]. A major advantage of lamellar phases, e.g., a SmB phase, presenting a single facet orientation is that stationary or, at least, permanent regimes can be observed in TDS as a function of the orientation of the crystals [8–10].

In TDS, the growth dynamics of a planarly oriented single crystal depends on the orientation of the facet plane with respect to the solidification axis, i.e., on the angle θ between the axis $\mathbf{z}$ of the thermal gradient and $\mathbf{n}_{\mathrm{Sm}}$ (Fig. 3)—note that $\theta = \phi + \phi_{z\zeta}$, where $\phi_{z\zeta}$ is the angle between $\mathbf{z}$ and the direction ζ of friction [10]. Very special, nonstationary patterns (not described here) are observed for θ within a few degrees of 0° or 90°. For all the other values of θ, there exist stationary and permanent patterns, the qualitative features of which are independent of θ.

At rest ($V=0$), the SmB-nematic interface of a single crystal is fully nonfaceted, and sits at a z position corresponding to T_{NS}. For V below the cellular threshold velocity V_c, the system reaches the stationary planar-front regime after a certain transient time (solute redistribution transient). The front then remains fully nonfaceted (Fig. 3). For $V > V_c$ ($V_c \approx 2.5 \mu\mathrm{m\,s^{-1}}$ for $G = 54\ \mathrm{K\,cm^{-1}}$), two kinds of patterns are observed, depending on boundary conditions,

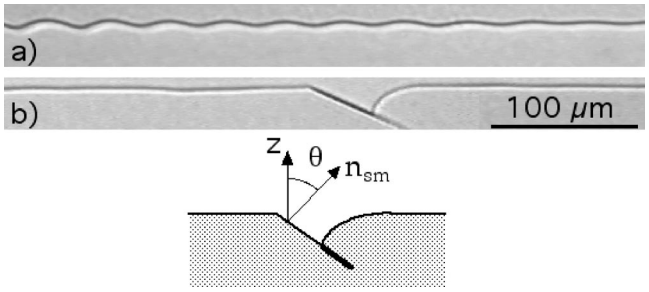

FIG. 5. Thin-sample directional solidification of CCH4 in a PTFE-coated sample ($G = 54\ \mathrm{K\,cm^{-1}}$). (a) Drifting shallow cells ($V = 3.1\ \mu\mathrm{m\,s^{-1}}$); (b) Stationary faceton ($V = 3.1\ \mu\mathrm{m\,s^{-1}}$). Sketch, definition of the angle θ (see text).

namely, nonfaceted patterns made of drifting shallow cells [Fig. 5(a)], and localized, dynamical objects, similar to traveling waves, called facetons because their existence is intrinsically bound to the presence of a facet which grows at a velocity v_n generally much smaller than $0.1V$ [Fig. 5(b)]. A faceton appears in most cases from a drifting-cell pattern, the amplitude of which is sufficient for a small portion of the smectic-layer plane to be exposed to the nematic. In a faceton, a clearly visible facet extends relatively deeply into the crystal. A thin nematic channel thus forms, which is necessarily faceted on both sides. A faceton either drifts at constant velocity along the front (''stationary'' faceton), or oscillates while drifting. That oscillation corresponds to a relaxation cycle of the facet between its blocked state and a state where it is growing. The regularity of the phenomenon inclines us to think that an instability of the nematic groove similar to the ''droplet instability'' observed in ordinary deep-cell patterns [34], is at the origin of that oscillation (Fig. 6).

Since a stringent requirement for observing steady TDS patterns is the selection of large, planarly oriented single SmB crystals of well-controlled in-plane orientation, we performed most of the TDS experiments in a series of PTFE-coated samples with different orientations of the friction axis, i.e., with different values of $\phi_{z\zeta}$. A counterpart of the use of PTFE-coated samples is that some defects in the nematic provoke a permanent perturbation of the SmB-nematic front, even for $V < V_c$ [10]. The major perturbation comes from the nematic-domain structure (see below). The fluctuations of the front are clearly slaved to the domain walls, which remain unperturbed even in the vicinity of the moving interface, and impose the scale of the perturbation (typically in the 100-μm range). More localized perturbations of the front (on a scale of the order of 10 μm) are due to individual

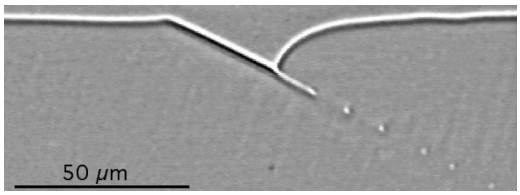

FIG. 6. The ''droplet instability'' of the thin groove of a drifting faceton (TDS; $G = 54\ \mathrm{K\,cm^{-1}}$; $V = 3.1\ \mu\mathrm{m\,s^{-1}}$).

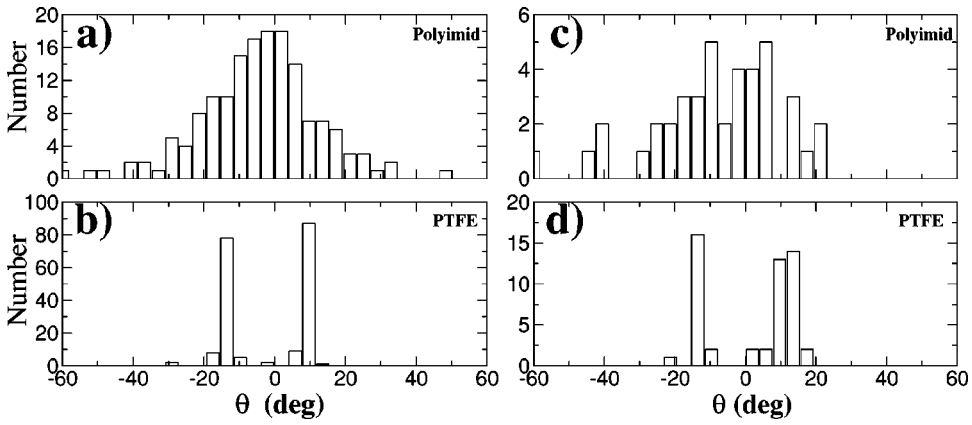

FIG. 7. Histograms of the final values of the disorientation angle ϕ of SmB crystals nucleated in PI-coated samples (a) and (c) and in PTFE-coated samples (b) and (d), in TFG (a) and (b) and in TDS (c) and (d).

defects in the nematic, most probably disclinations. These defects are mobile, contrary to domain walls. They are generally not destroyed when meeting the front, but rather migrate along the interface (in the manner of a dust particle) until they collapse with another defect of opposite sign.

IV. RESULTS

A. Nucleation, isothermal growth and recrystallization process

1. PI-coated samples

We measured the disorientation angle ϕ for about 200 SmB crystals nucleated in two different PI-coated samples. The ϕ distribution, shown in the histogram of Fig. 7(a), is a broad symmetric peak centered onto zero. This is in full agreement with previous results [3]. The same qualitative features were also observed for CCH3 and CCH5, but the width of the ϕ distribution was much narrower (respectively, broader) for CCH3 (respectively, CCH5) than for CCH4. A similar distribution [Fig. 7(c)] is observed in TDS when SmB crystals nucleate ahead of the front (see below).

The values of ϕ reported in Fig. 7(a) were measured in well-developed crystals. In fact, the final orientation of a large crystal is often different from that of the initial nucleus, i.e., the orientation of the crystal changes during growth. Figure 8(a) shows successive stages of the growth of a SmB crystal with a large initial disorientation ($\phi \approx 60°$). A plot of ϕ as a function of time t [Fig. 8(b)] reveals that the crystal starts rotating after a delay time of a few 0.1 s, its characteristic dimension being then of about 10 μm. It stops rotating (but not growing) when its (largest) dimension is about 80 μm. The whole process occurs within about 1.5 s. This phenomenon may be explained as follows. As long as $\phi \neq 0$, an elastic torque is applied to the crystal because of the distortion of the nematic around it, whence its rotation motion. The existence of a delay for the rotation shows that the nucleus sticks initially to one of the sample walls. The final ϕ value, which is far from being zero, corresponds to the time at which the crystal fills the thickness of the sample. Interestingly enough, the alignment of such a crystal along ζ can be completed by remelting it partly so that it reaches a typical size less than 10 μm.

The rotation of the crystal (analog to that of a damped torsion pendulum) results from a combination of elastic forces, viscous flow and inertial forces in a time dependent geometry. This complex problem is not addressed here. We simply note that the thin nematic layers squeezed between the crystal and the glass plates are extremely distorted, while the distortion near the other faces of the crystal must be smoother. Therefore, it may be conjectured that elastic forces, but also friction forces, strongly depend on the shape, i.e., on the aspect ratio, of the growing crystal.

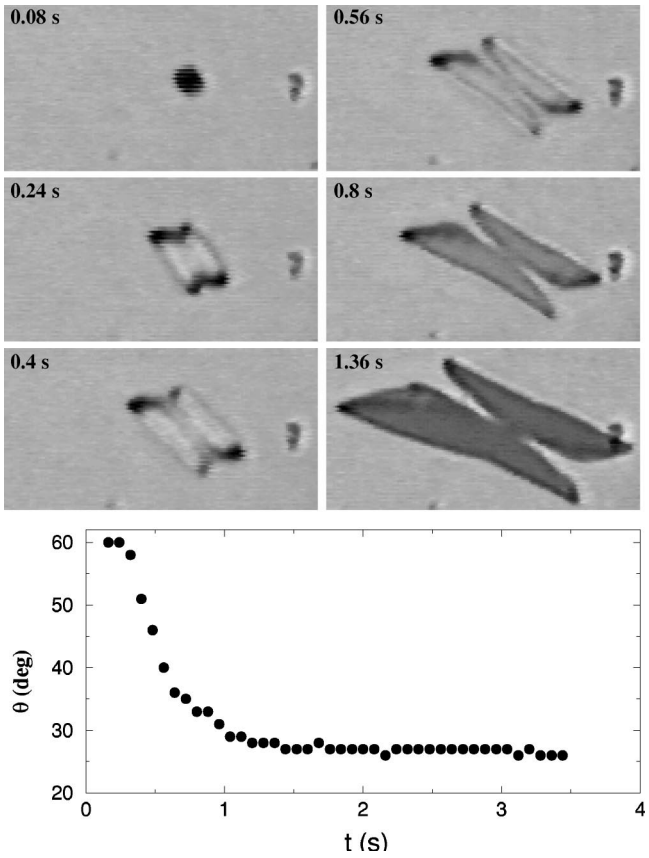

FIG. 8. Rotation of a highly misoriented SmB crystal of CCH4 nucleating and growing in a PI-coated sample. Top, successive stages of the growth of the crystal. Horizontal dimension of each snapshot, 120 μm. Bottom, graph of the disorientation angle ϕ of the crystal as a function of time t. The first point was measured when the size of the crystal was of about 10 μm.

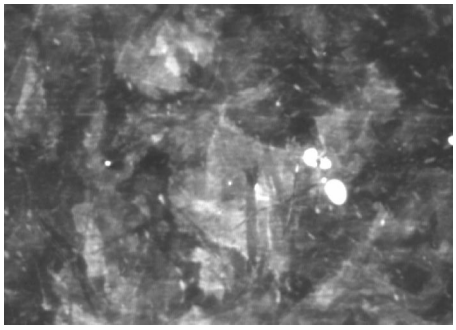

FIG. 9. Nematic phase in a PI-coated sample initially maintained at room temperature (it was then a SmB polycrystal) several weeks and heated up again to $T > T_{NS}$. The rubbing axis ζ is horizontal. Crossed polars. The optical contrast due to a memory effect in the nematic was much enhanced numerically, and corresponds to very slight variations of the orientation of the nematic director. Horizontal size: 420 μm.

The above observations (the broadness of the disorientation distribution, and the rotation of highly disoriented crystals during growth) show that, in PI-coated samples, the orientation of SmB crystals is not principally determined by specific interactions with the polymer film, but by elastic interactions with the surrounding nematic. This clearly explains why the orientation effect is weak. Probably, the planar orientation is determined by the same mechanism. Apparently, the planar-orienting effect is more efficient than the in-plane one (the reason for this remains unclear), but SmB crystals with an imperfect planar alignment are also occasionally observed ($\mathbf{n}_{\mathrm{Sm}}$ is then tilted with respect to the sample plane).

We gain more information on the interactions between the CCH4 molecules and the PI film by observing the structure of the nematic in a PI-coated sample after remelting the SmB polycrystal. By melting a fully crystallized PI-coated sample a short time after a first solidification, the nematic phase recovers a uniform alignment, even after several crystallization runs (see the nematic surrounding the SmB crystal of Fig. 8). A ''memory effect'' is observed only when the sample is maintained in the SmB state (at room temperature) several weeks long: the nematic is then structured into domains of different alignment and containing many defects (Fig. 9). However, the correspondence between the grain structure of the initial SmB polycrystal and the nematic domain structure is not clear. The misalignment angle within each domain is small: the main alignment effect remains that of the roughness of the PI film. The existence of a memory effect evidences the existence of an adsorption layer of CCH4 onto the PI film. However, in ordinary experimental conditions, this adsorption layer is probably disordered and has a weak effect on the crystallization process. It will be seen presently that the situation is completely different in PTFE-coated samples.

2. PTFE-coated samples

In PTFE-coated samples, nucleation is observed for relatively small values of the undercooling (>0.1 K). Accordingly, the density of SmB nucleation sites is larger than in PI-coated ones, for a given undercooling. The SmB crystals are closer to each other, and the dendritic patterns are smaller and less branched (Fig. 10) than, but similar in shape to crystals observed in PI-coated samples. On the other hand, the crystals are systematically tilted with respect to the average nematic orientation ζ with reproducible disorientation angles $\pm\phi_{\mathrm{PTFE}}$, where $\phi_{\mathrm{PTFE}} = 13° \pm 1°$. Positive and negative ϕ values are observed in equal number. The tails of the distribution [Fig. 7(b)] are essentially due to crystals nucleated onto isolated defects of the PTFE films (we did not take the crystals nucleated in highly perturbed regions into account). Thus, just after the completion of the solidification, a SmB polycrystal of CCH4 in a PTFE-coated sample contains a large number of grains with disorientation angles of $\pm\phi_{\mathrm{PTFE}}$, and a few grains of arbitrary orientations. Again, a similar distribution is observed in TDS (Fig. 7d). We return to this phenomenon in Sec. IV B.

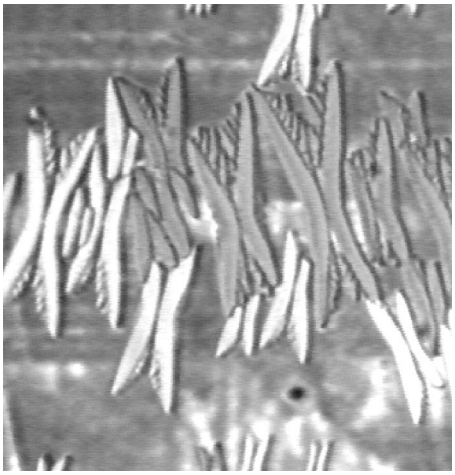

FIG. 10. Thin-sample free growth ($\Delta T \approx 0.4$ K). Smectic-*B* crystals of CCH4 growing in a 12-μm thick PTFE-coated sample filled *in situ* (method 1). The nematic phase is aligned uniformly along the horizontal friction axis, except for some defects appearing as straight thin lines. Horizontal dimension: 860 μm.

The memory effect is much stronger in remelted PTFE-coated samples than in PI-coated ones. By remelting a once solidified PTFE-coated sample of CCH4 [Fig. 11(a)], one obtains a planar nematic phase, which is now structured into domains [Fig. 11(b)]. Each nematic domain appears uniformly oriented between crossed polars. The nematic orientations differ from one domain to another, and the angle ϕ_{nd} (where *nd* stands for nematic domain) between ζ and $\mathbf{d}$, which was initially equal to zero, takes on values intermediate between zero and $\pm\phi_{\mathrm{PTFE}}$ (we measured values between 5° and 10°). The domains are separated from each other by sharp (within thermal fluctuations) boundaries, which more or less coincide with the grain boundaries (GBs) of the polycrystal. When such a ''marked'' sample is cooled down again to a temperature below T_{NS}, SmB crystals nucleating within a given nematic domain are all of the same orientation [Fig. 11(b)]. The corresponding value of ϕ is close (within 1°) to that of the previously grown SmB crystal. These facts explain the existence of a nematic-domain structure in PTFE-

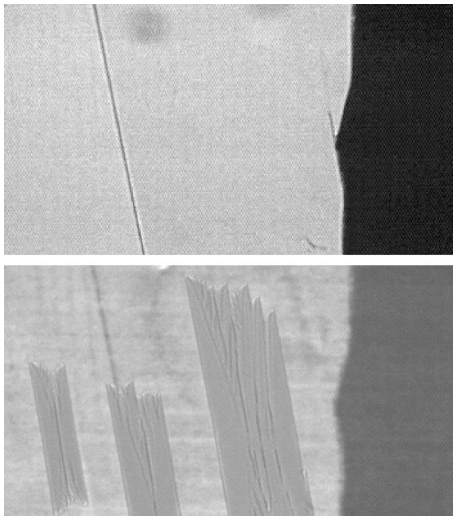

FIG. 11. PTFE-coated sample of CCH4. Crossed polars. The friction axis ζ is vertical. (a) Fully crystallized smectic-*B* (TFG; $\Delta T \approx 0.2$ K). The three crystals visible in the image are larger than the field of view. The two crystals on the left part of the image have nearly the same in-plane orientation; (b) same sample first heated above T_{NS}, and then cooled down again below T_{NS}. The nematic domains roughly coincide with the previous SmB grains. A few SmB crystals which renucleated during the cooling are also visible. Horizontal dimension: 570 μm.

coated samples prepared by method 2.

The history-dependent domain structure of the nematic does not disappear when T is increased to values slightly higher than T_{NS}. This signals that CCH4 molecules strongly adsorb onto the PTFE film. The strength of the adsorption is evidenced by the fact that nematic domains reappear after the sample has been maintained overnight at $T \approx 90\,^{\circ}$C, thus in the isotropic state, and cooled down again below T_{IN} (but slightly above T_{NS}). However, the domain boundaries appear then much blurred, and the nematic alignment is no more uniform within a given domain. Moreover, it seems that the value of ϕ_{nd} within each domain is somewhat closer to zero.

The above observations strongly suggest that the epitaxy process at play in PTFE-coated samples of CCH4 does not occur directly onto the PTFE film itself, but onto a layer of CCH4 molecules, which has adsorbed when the nematic first entered into contact with the PTFE film. This is a case of homoepitaxy of SmB crystals onto a crystalline layer of CCH4 molecules, the structure of which is not necessarily that of a stable bulk phase (a similar phenomenon was observed in thin films of another liquid-crystal molecule, called 8CB, classically used as a model mesogenic system, deposited onto the flat surface of a MoS_2 single crystal, at a temperature close to that of the nematic-smectic-*A* transition of the bulk 8CB [35]). The homoepitaxy phenomenon does definitely not exist with PI. The two degenerate planar orientations $+\phi_{\mathrm{PTFE}}$ and $-\phi_{\mathrm{PTFE}}$ of the macroscopic SmB crystals in PTFE-coated samples must result from a specific lattice matching between the thin adsorbed layer and the bulk SmB phase occurring for those values of ϕ. That the adsorbed layer does not determine the alignment of the nematic in freshly filled samples suggests that the crystalline layer is made of a large number of very small grains of different orientations, or contains a large number of defects. It may also be conjectured that those defects could be induced by the structure of the PTFE film, that is, either by an irregular topography on a microscopic scale, or by defects specific of the helix structure of the PTFE chains. As long as the adsorbed layer is disordered on a scale comparable to that of the fluctuations of the nematic order, the bulk nematic is insensitive to it and is aligned along an average direction imposed by the microscopic roughness of the film, which is a symmetry axis of the system. As the growth of bulk SmB crystals occurs, the adsorbed layer undergoes a reorganization over long distances, which breaks the initial axial symmetry about the direction of friction, and modifies the anchoring of the nematic. The fact that the nematic appears uniform within each domain signals that the upper and the lower surface layers (adsorbed on the upper and the lower glass walls of the sample) are identically reorganized. The ordered structure of the surface layers is not much perturbed after remelting, as evidenced by the strong memory effect. The fact that $|\phi_{nd}|$ takes intermediate values between ϕ_{PTFE} and zero may be the sign of a competition, in the nematic alignment effect, between the roughness of the PTFE film and the order of the adsorbed layer. When the sample is heated up to the isotropic phase, either a slow desorption of the molecules occurs, or, more probably, the adsorbed layer only undergoes a slow disordering.

3. Recrystallization process

In a PTFE-coated sample, the grain structure of a polycrystal sample grown in TFG and maintained at a ΔT value smaller than 0.3 K (the SmB grains are then in a small number, thus of large size) does not evolve in time—such was the case in Fig. 11. For $\Delta T > \Delta T_{recryst} \approx 0.3$ K, the polycrystal undergoes a recrystallization process, during which some grain boundaries, or some parts of them, migrate, generally in a stepwise manner (Fig. 12). The normal velocity of a grain boundary can reach a few 10 $\mu\mathrm{m\,s}^{-1}$. A transient three-dimensional (3D) deformation of the GB is sometimes observed, which evidences a marked sensitivity to the roughness or chemical heterogeneities of the substrate, like in a wetting process. The process is rapid during the first 10 s, and then slows down. It is essentially completed within 1 min.

The domain structure of the nematic phase after the melting of a recrystallized sample keeps memory of both the SmB grain structures before and after the recrystallization process, even after a long stay at an undercooling larger than $\Delta T_{recryst}$, and becomes very complex. This probably means that the recrystallization process affects only one of the two (upper and lower) adsorbed layers. Therefore, after a recrystallization process, the two inner surfaces of the sample are no longer identical, and the orientation within nematic domains does not simply reflect that of the adsorbed layers. This is evidenced by the fact that both $+\phi_{\mathrm{PTFE}}$ and $-\phi_{\mathrm{PTFE}}$ disorientation angles of SmB crystals nucleated in a remelted (once recrystallized) sample are observed within a given nematic domain (Fig. 13).

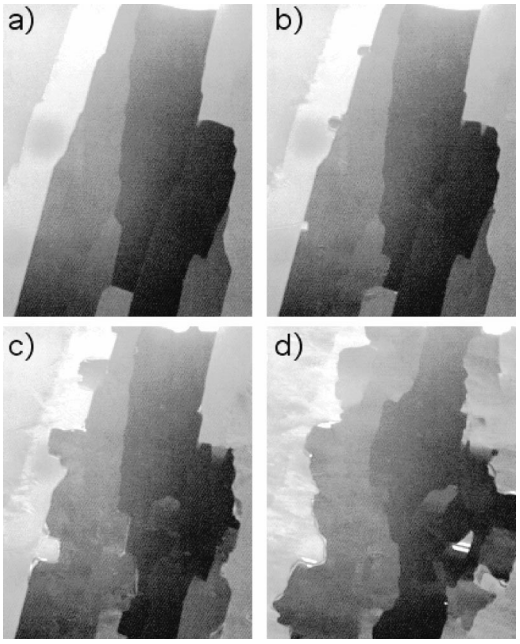

FIG. 12. Recrystallization phenomenon in a PTFE-coated sample of CCH4 (TFG; $\Delta T \approx 0.4$ K). The friction axis ζ is vertical. Crossed polars. (a) $t=0$ (the crystallization is complete); (b) $t=4$ s; (c) $t=7$ s; (d) $t=48$ s. Horizontal dimension of each snapshot: 370 μm.

In TDS, the recrystallization process takes the form of a ''second front'' following the nematic-SmB front at fixed distance corresponding roughly to $\Delta T_{recryst}$ (Fig. 3; also see Fig. 19 below). A more intriguing configuration, in which the recrystallization front bends itself to join the nematic-SmB front [see Fig. 16(a) below] is also frequently observed. Such a configuration is not in equilibrium, but drifts laterally as a whole in a direction corresponding to the decrease of the size of the high-temperature grain [i.e., leftwards in the case of Fig. 16(a)]. These observations can be explained qualitatively in the frame of a first-order transition scheme. The two different ''phases'' (in the definition of which surface effects must be included) are in equilibrium at a definite temperature $T_{eq}=T_{NS}-\Delta T_{recryst}$. The migration observed in Fig. 16(a) means that the gain in bulk free energy due to the presence of the high-temperature phase above T_{eq} is less than the loss due to the presence of the recrystallization front—in other words, the high-temperature grain has a subcritical size. However, the quantitative details, especially the fact that, in Fig. 16(a), there is no measurable temperature difference between the $G1$-liquid and $G2$-liquid interfaces, pose problems. At present, the question of the nature of the driving force responsible for the recrystallization process remains open.

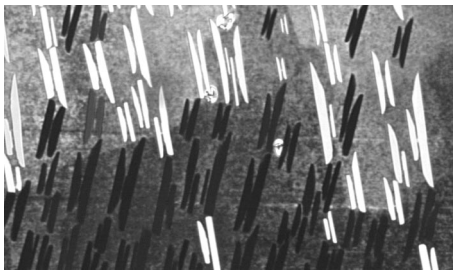

FIG. 13. Nucleation of SmB crystals in a PTFE-coated sample of CCH4 (TFG; $\Delta T \approx 0.4$ K). The nematic-domain structure is inherited from a first solidification and an isothermal recrystallization process in the SmB state. The friction axis ζ is vertical. Crossed polars. Horizontal dimension, 1.2 mm.

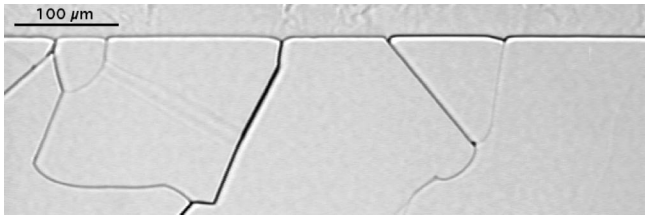

FIG. 14. The nematic-SmB interface of a CCH4 polycrystal in a PTFE-coated sample at rest ($V=0$) in TDS. End of the coarsening process.

B. Faceting and nucleation in directional solidification

1. Nonfaceted and faceted GB grooves at rest (V=0)

In the PTFE-coated samples that we use in directional solidification, most of the grains exhibit a disorientation angle close to $\pm\phi_{\mathrm{PTFE}}$. Due to nucleation onto defects of the PTFE films, some grains markedly misoriented with respect to the epitaxy angles are also present. At rest in the thermal gradient, the nonmelted part of such a polycrystal sample undergoes a grain coarsening process, which affects the solid far below T_{NS}. In contrast to the recrystallization process described above, which occurs below a threshold temperature lower than T_{NS}, the considered coarsening process is particularly active near the solid-liquid interface. There, GBs are highly mobile, and rearrange in order to intersect the solid-liquid interface at right angle. The motion of the GBs slows down progressively, and, after several tenths of minutes, GBs have practically ceased moving (Fig. 14). The typical distance between GBs intersecting the front (grain size) is then of a few 100 μm. At this stage, the nematic-SmB interface is planar except for a few shallow grooves (or cusps) attached to GBs.

In the vicinity of the SmB-nematic interface, GBs run perpendicular to the sample plane, and parallel to **z**. This (and the high mobility of the GBs) shows that the GBs are ''wetted'' by the nematic (an exception to this rule corresponds to GBs running parallel to the smectic-layer plane of one of the adjacent grains, indicating a singularity of the Wulff plot of the GBs in that orientation; one of such GBs is visible in Fig. 14). Let θ_1 and θ_2 be the disorientation angles of two adjacent grains $G1$ and $G2$, respectively (Fig. 15). The surface tension γ_{GB} of a GB such that the value of the angle $\theta_{12}=\theta_1-\theta_2$ (which is one of the angular components characterizing the misorientation of the GB) is larger than a few degrees, is equal to $2\gamma_{NS}$ [36]. The apex angle between the two solid-liquid interfaces on the bottom of a GB groove is zero (Young's law). Let us consider the case $\theta_1<0$ and $\theta_2>0$. Then, the smectic-layer plane is not exposed to the

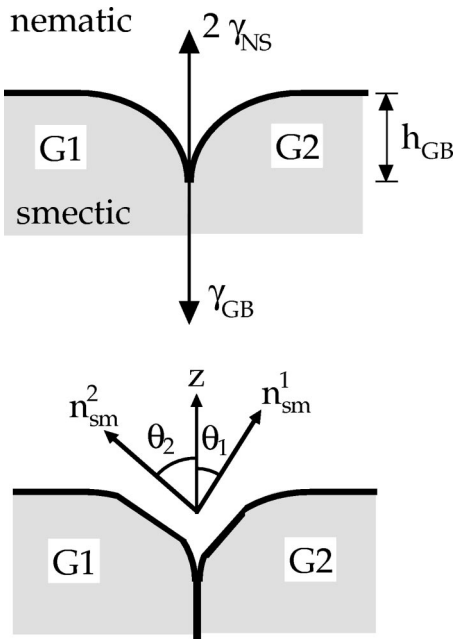

FIG. 15. Grain boundary grooves (sketches). Top, nonfaceted groove. Bottom, faceted groove.

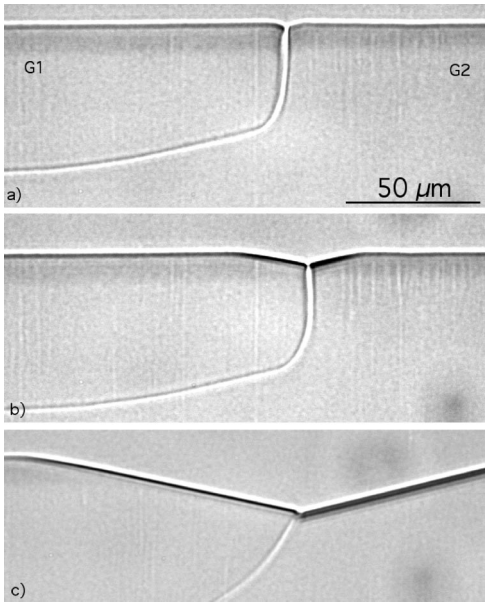

FIG. 16. A symmetric faceted GB groove in a CCH4 polycrystal in a PTFE-coated sample in TDS: (a) at rest ($V=0$); (b) during the solute redistribution transient ($V=2\ \mu\mathrm{m\,s^{-1}}$); (c) V-shaped GB groove pattern.

nematic, and the GB groove is fully nonfaceted. A rough estimate of γ_{NS} can be obtained by measuring the depth h_{GB} of the groove, and using the fact that, for a wetted GB in an isotropic system, h_{GB} is equal to a capillary length $d_c=\sqrt{2a_o/G}$ ($a_o=\gamma_{NS}T_m/L_v$ is the Gibbs-Thomson coefficient, T_m is the melting temperature of the pure system, and L_v is the latent heat per unit volume), which is also the length over which the GB groove extends along the direction **x** [37]. We measured directly $h_{GB}\approx 3\ \mu$m (within $\pm 1\ \mu$m) for $G=54\ \mathrm{K\,cm^{-1}}$, thus $a_o\approx 2.5\times 10^{-8}\ \mathrm{K\,m}$, which gives $\gamma\approx 3\ \mathrm{mN\,m^{-1}}$ ($L_v\approx 44\ \mathrm{J\,cm^{-3}}$). This is a reasonable value for such a system.

At rest, a GB groove can be faceted either on both sides if $\theta_1>0$ and $\theta_2<0$, or on one side only if θ_1 and θ_2 are of the same sign. The facets are generally hardly visible when the front is strictly at rest [Fig. 16(a)]. On the other hand, if the front slightly advances, either because of an accidental perturbation of the thermal field, or of a slow drift of the grain boundary along the front, the facets appear clearly (Fig. 14). This is a further evidence of the fact that the facets remain blocked at small undercoolings.

2. Grain selection mechanism

The drifting motion of asymmetric GB groove patterns is the main ingredient of a grain selection mechanism at play in PTFE-coated samples. It is therefore worth studying the mechanisms of drift of the GB grooves in some detail. Several cases corresponding to different signs of θ_1 and θ_2 must be considered in turn. When a GB groove is nonfaceted ($\theta_1<0$ and $\theta_2>0$), its shape does not change significantly, and the large-scale dynamics of the front is not disturbed at low velocity ($V<V_c$). On the other hand, for $V>V_c$, a precursory deformation of the front in the vicinity of the GB groove serves as an initiator for the cellular instability, as it is generally observed in TDS experiments [38].

When a GB groove is faceted, it starts to deepen from the onset of the pulling. The preexisting facets extend continually during the solute redistribution transient [Figs. 16(b) and 16(c)]. They recoil first at a velocity nearly equal to $-V$, i.e., they do not, or almost not grow. When the undercooling of the coldest end of the facets reaches a value of about 0.1 K, they start growing, and the deepening of the GB groove slows down.

When the GB groove is faceted on one side only (θ_1 and θ_2 of the same sign), a localized, permanent pattern forms, which drifts along the front. If $V<V_c$, the groove remains faceted on one side only, the drifting motion is governed by that of the facet, and the nonfaceted side of the pattern slightly bulges in the nematic towards the drifting direction (Fig. 17). The pattern is then very similar to a faceton locked onto a GB (''GB-locked faceton''), and drifts laterally at a constant velocity. A GB formed by this mechanism is tilted in the solid with an angle which is determined by the drift of the GB groove pattern. In some cases, the other facet, that

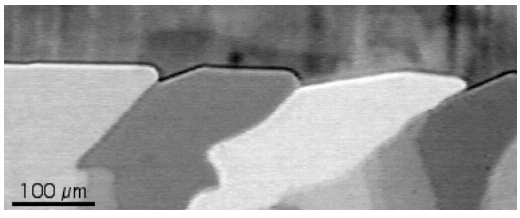

FIG. 17. Faceted patterns (GB locked facetons) attached to GBs in TDS ($V=3\ \mu\mathrm{m\,s^{-1}}$) of a CCH4 polycrystal (PTFE-coated sample). These patterns drift along the front, as evidenced by the tilt of the GBs in the solid.

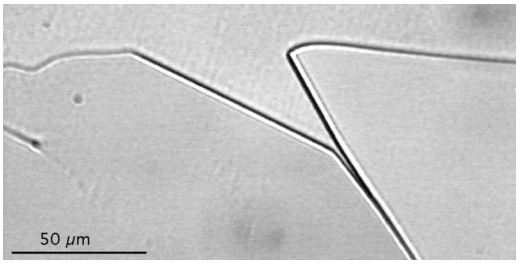

FIG. 18. A fully faceted (drifting) pattern attached to a GB in TDS of a CCH4 polycrystal (PTFE-coated sample).

did not form at rest for geometrical reasons, appears, which results in a pattern such as that shown in Fig. 18.

The grooves that are faceted on both sides ($\theta_1>0$ and $\theta_2<0$) can be either symmetrical ($\theta_1=-\theta_2$) or asymmetrical ($\theta_1\neq-\theta_2$). The latter drift laterally, whereas the former do not drift. In PTFE-coated samples with the PTFE friction axis ζ perpendicular ("$\perp$ samples") or parallel ("$\parallel$ samples") to **z**, most, but not all, crystals are "well oriented," i.e., their in-plane orientation is such that $|\theta|$ is close to ϕ_{PTFE} and to $\pi/2-\phi_{\mathrm{PTFE}}$ in $\parallel$ and $\perp$ samples, respectively. In the first stages of the solidification run, the drift of asymmetric GB grooves and of GB-locked facetons leads to the elimination of most of the misoriented grains, while well-oriented grains extend laterally. This leads to the elimination of the few grains that have a disorientation angle different from $\pm\phi_{\mathrm{PTFE}}$. Grains of positive and negative θ values then alternate ($\theta_1\approx-\theta_2$), and are separated either by nonfaceted grooves or by faceted GB grooves with a symmetric shape, called "*V*-shaped" patterns [Figs. 19(a) and 20]. The angle between two adjacent facets is equal to about $2\phi_{\mathrm{PTFE}}$ ($\pi-2\phi_{\mathrm{PTFE}}$) in $\perp$ ($\parallel$) samples. For $V<V_c$, *V*-shaped patterns are essentially stationary. The average normal velocity of the facets is then $V\cos\theta$. We will see later on that the growth of the facets is in fact irregular on a short time scale.

The depth *h* of *V*-shaped patterns does not depend much on *V* when $V<V_c$. It is comparable to that of a faceton when *V* is close to V_c, and increases with $V>V_c$. It is typically 60 μm for $G=54\ \mathrm{K\,cm^{-1}}$ ($V_c\approx8\ \mu\mathrm{m\,s^{-1}}$) and *V*

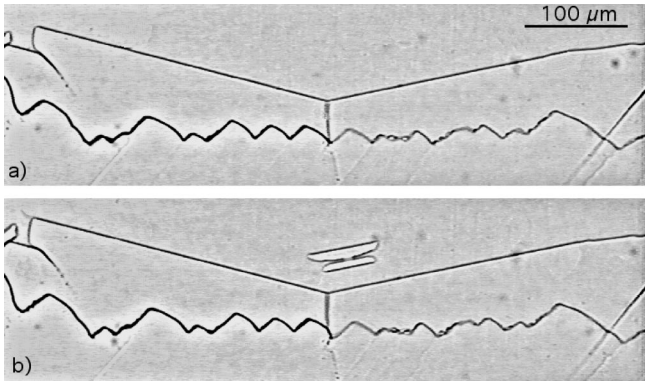

FIG. 19. Obtuse V-shaped faceted pattern attached to a GB in TDS of a CCH4 polycrystal in a PTFE-coated sample with friction axis parallel to the solidification one ($V=14\ \mu\mathrm{m\,s^{-1}}$). (a) Stationary pattern; (b) nucleation of a new crystal.

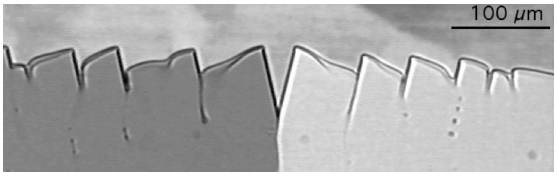

FIG. 20. Stationary acute V-shaped faceted pattern attached to a GB in TDS of a CCH4 polycrystal in a PTFE-coated sample with friction axis perpendicular to the solidification one ($V=14\ \mu\mathrm{m\,s^{-1}}$).

$=14\ \mu\mathrm{m\,s^{-1}}$, which corresponds to an undercooling in the bottom of the pattern of about 0.5 K (for such *V* values, the whole front is composed of faceted fingers, typical of the high-velocity regime [10]). This is potentially sufficient for nucleation to occur within the nematic trough bordered by the facets. Nucleation events are indeed observed in "obtuse" ($\theta_1=-\theta_2=\phi_{\mathrm{PTFE}}$) *V*-shaped grooves [Fig. 19(b)] in $\parallel$ samples.

The phenomenon of nucleation of crystals ahead of the solidification front is a common one in directional solidification above the cellular threshold [9]. The frequency of the nucleation events depends on the density of nucleation sites n_s, which is small in the present system (the time lapse between two successive nucleation events is of several seconds for $V=14\ \mu\mathrm{m\,s^{-1}}$). Remarkably enough, no nucleation events are observed in "acute" ($\theta_1=-\theta_2=\pi/2-\phi_{\mathrm{PTFE}}$) *V*-shaped grooves ($\perp$ samples). This is due to the fact that, as nucleation sites active for ΔT values smaller than 0.3 K are rare, as shown by TFG experiments, the extension of the nematic region bordered by the facets in acute *V*-shaped troughs is too small (much smaller than in the obtuse ones) for nucleation to occur. By estimating the flux *f* of nucleation sites through a *V*-shaped pattern as being equal to $2Vn_sh/\tan(\phi_{\mathrm{PTFE}})$ for an obtuse pattern and $2Vn_sh/\tan(\pi/2-\phi_{\mathrm{PTFE}})$ for an acute one, one finds that the ratio between the two values of *f* is equal to $\tan(\pi/2-\phi_{\mathrm{PTFE}})/\tan(\phi_{\mathrm{PTFE}})\approx20$, which agrees well with the proposed explanation.

In an obtuse *V*-shaped pattern, each new crystal grows rapidly (within several 0.1 s) in conditions approximately similar to a free-growth configuration with a regularly increasing undercooling. It thus fills rapidly the lowest part of the groove. As expected from observations in TFG, the disorientation angle of crystals nucleating in *V*-shaped troughs is generally $+\phi_{\mathrm{PTFE}}$ or $-\phi_{\mathrm{PTFE}}$ [Fig. 7(d)], according to the nematic domain within which they appear. At the end of the nucleation and growth process, the new crystal is practically undistinguishable from one of the two preexisting neighboring grains, and no GB is formed, if ϕ is strictly equal to $\pm\phi_{\mathrm{PTFE}}$. When a GB (or a subboundary) forms, it is highly asymmetric, and thus drifts rapidly along the front. When the new grain meets the previous grain of opposite orientation, an obtuse *V*-shaped groove is restored. This groove starts then to deepen again, and the whole process can reiterate cyclically (Fig. 21).

Finally, several phenomena—the epitaxy of SmB crystals nucleating during solidification, the lateral drift of GBs between misoriented grains and the fact that symmetric pat-

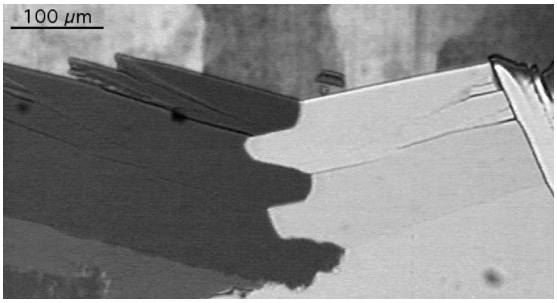

FIG. 21. Reiterated nucleation events in an obtuse V-shaped faceted pattern attached to a GB in TDS of a SmB polycrystal in a PTFE-coated sample of CCH4 with friction axis parallel to the solidification one ($V=14\ \mu\mathrm{m\,s^{-1}}$).

terns associated to well-oriented grains are stationary or cyclically restored—work towards a grain selection mechanism in $\parallel$ and $\perp$ PTFE-coated samples. Only a major disturbance (e.g., the nucleation of markedly misoriented crystals onto defects or the meeting of the recrystallization front with the bottom of a GB groove) may lead to the destruction of the thus selected polycrystal.

3. Facet growth and formation of grain subboundaries

In a polycrystal sample, there are not only GBs of large misorientation, but also grain subboundaries (SBs). A SB is made of a regular arrangement of dislocations. Its surface tension γ_{SB} is less than $2\gamma_{NS}$, and decreases when the misorientation decreases—it is more or less proportional to the misorientation angle θ_{12}. Accordingly, the depth h_{SB} of the groove created by a SB emerging at the solid-liquid interface is less than d_c.

The presence of SBs is clearly revealed during a solidification run, because, as a SB groove slightly deepens, a small facet appears systematically on one side of it. The depth of such a SB groove—thus the size of the facet—is small (it does not exceed a few micrometers), and the facet remains in a blocked state. Consequently, SB grooves drift laterally along the front at a constant speed equal to $V/\tan\theta$. The SB left in the solid is tilted with an angle equal to θ and is parallel to the smectic plane of one of the grains.

We observed that a relatively large number of SB grooves permanently sweep the front during a long-time solidification run. As they drift, they are necessarily eliminated when they meet one edge of the sample (or a GB). Therefore, there must exist a mechanism of creation of SBs during growth. We did not observe the polygonization during growth described recently by Bottin-Rousseau *et al.* [39] in TDS of nonfaceted organic crystals. In the CCH4 system, SBs are emitted from the large facets attached to the GBs, as it will be explained presently.

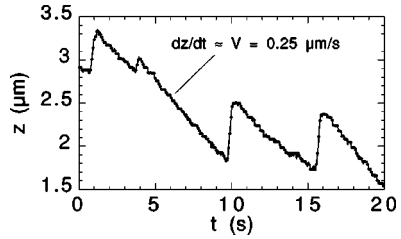

FIG. 22. The z position of the front at a fixed coordinate $x=50\ \mu$m within the facet of grain G1 of Fig. 16 as a function of time t at the end of the transient recoil of the nonfaceted part of the front.

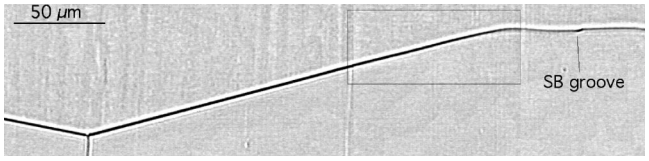

FIG. 23. Large V-shaped faceted GB groove in a PTFE-coated sample (TDS; $G=54\ \mathrm{K\,cm^{-1}}$; $V=3\ \mu\mathrm{m\,s^{-1}}$). The friction axis ζ is parallel to the solidification axis z. A small facet drifting laterally towards the right side of the sample, signals the presence of a SB. Frame, region analyzed in Fig. 24.

The growth of facets bordering a V-shaped pattern attached to a symmetric GB occurs in a stepwise manner. This can be seen by recording the z position of a point of the facet (at fixed x) as a function of time t (Fig. 22). Most of the time, the facet recoils towards the cold part of the setup at a velocity close to V. It is thus in a (nearly) blocked state. At time intervals of a few seconds (for V in the $1\text{-}\mu\mathrm{m\,s^{-1}}$ range), the facet seems to progress very rapidly (within much less than 1 s) towards the liquid. In fact, this corresponds to the motion of a macrostep along the facet.

The process of creation and propagation of macrosteps is illustrated in Figs. 23 and 24. In Fig. 23, one can see the right part of a large, stationary V-shaped GB groove pattern. We have recorded the shape of the SmB-nematic interface in the region delimited by the frame in that figure as a function of time. Three profiles corresponding to successive times are shown in Fig. 24. In that figure, the average slope of the facet is subtracted from the interface shape, so that local departures from a flat facet are emphasized. Time $t=0$ was chosen at a moment when the facet was nearly blocked and is approximately flat, except in the region where it joins the rough part of the SmB-nematic interface. At time t_1, a small bump appears on the left part of the figure, at some position x. About one second later (time t_2), that bump has transformed into a macrostep of an amplitude of about 1 μm which propagates along the facet. The macrostep changes its shape

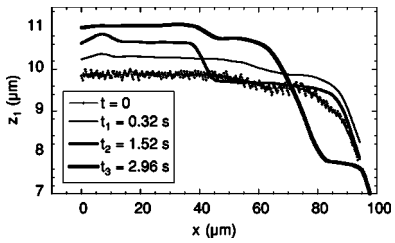

FIG. 24. Shape $z_1(x)$ of the moving nematic-SmB interface in the vicinity of the edge of the V-shaped pattern of Fig. 23 at successive times. The average slope of the facet has been subtracted to the $z(x)$ curves. The curves have been shifted apart from each other by an arbitrary value for the sake of clarity. Data points are shown for the curve at $t=0$.

and increases in amplitude as it progresses, but the advancing speed of its foremost point is approximately constant. At time t_2, a new bump has appeared at the rear of the macrostep, at the same place as the former one. When a macrostep reaches the external edge of the *V*-shape pattern, thus the planar, rough part of the growth front, it quite systematically emits a very small drifting facet, such as that shown in Fig. 23.

Our observations give a clear evidence that the main mechanism of faceted growth in CCH4 is the propagation of steps from terraces nucleating onto preferential sites, and undergoing a bunching instability leading to the formation of macrosteps. Small bumps appear, repetitively, as precursors of the macrosteps at one and the same x position. We have observed that phenomenon many times. This means that preferential sites of terrace nucleation are situated onto the PTFE film, and are aligned along ζ. Those sites are probably of the same nature as the crystal nucleation sites. The point that we want to emphasize here is that terrace nucleation events, which are followed by the appearance of a macrostep, most probably correspond to cases where nucleation occurs with a slight misorientation. In other words, the emission of small facets drifting along the rough part of the front is the signature of a planar lattice defect associated to the formation of macrosteps. Those defects do not produce any detectable optical contrast when observed between crossed polars. They thus may be stacking faults, which are known to be easily created in a SmB phase, or SBs associated to an out-of-plane misorientation, i.e., a slight rotation about the normal to the smectic layers (variation of the angle α defined above), which is the optical axis of the SmB crystal. The latter one is the most plausible one, since the size of the small drifting facets is not a constant (it depends on the misorientation of the SB).

V. CONCLUSION

We have studied the mechanisms of crystal orientation in solidification experiments in thin samples of a mesogenic substance, CCH4, which undergoes a phase transition between a nematic and a smectic B. We have shown that the nature and the efficiency of those mechanisms depend much on the nature of the nucleation substrate, namely, a polymer film coating the inner surface of the glass-wall container. The use of samples coated with mono-oriented PTFE films leads to unexpected phenomena of grain selection and of generation of lattice defects in thin-sample directional solidification. A better understanding of those mechanisms would require the use of techniques of investigations on a microscopic scale.

ACKNOWLEDGMENTS

We would like to thank Á. Buka and T. Tóth-Katona for providing the CCH4. We benefited from fruitful discussions with M. Brunet and M. Schott. We thank G. Faivre for his critical reading of our manuscript. One of us (T.B.) benefited financially from the European Community program IMPROVING HUMAN POTENTIAL under Contract No. HPMF-CT-1999-00132.

[1] J. Cognard, Mol. Cryst. Liq. Cryst. Suppl. 1, **78**, 1 (1982).
[2] P.-G. de Gennes and J. Prost, *The Physics of Liquid Crystals* (Oxford University Press, New York, 1993).
[3] T. Tóth-Katona, T. Börzsönyi, Z. Váradi, J. Szabon, Á. Buka, R. González-Cinca, L. Ramirez-Piscina, J. Casademunt, and A. Hernández-Machado, Phys. Rev. E **54**, 1574 (1996).
[4] R. González-Cinca, L. Ramirez-Piscina, J. Casademunt, A. Hernández-Machado, T. Tóth-Katona, T. Börzsönyi, and Á. Buka, Physica D **99**, 359 (1996).
[5] T. Tóth-Katona, N. Éber, and Á. Buka, Mol. Cryst. Liq. Cryst. **328**, 467 (1999).
[6] T. Börzsönyi, T. Tóth-Katona, Á. Buka, and L. Gránásy, Phys. Rev. E **62**, 7817 (2000).
[7] T. Tóth-Katona, T. Börzsönyi, Á. Buka, R. González-Cinca, L. Ramirez-Piscina, J. Casademunt, A. Hernández-Machado, and L. Kramer, Phys. Rep. **337**, 37 (2000).
[8] P. Oswald, F. Melo, and C. Germain, J. Phys. (France) **50**, 3527 (1989).
[9] F. Melo and P. Oswald, J. Phys. II **1**, 353 (1991).
[10] T. Börzsönyi, S. Akamatsu, and G. Faivre, Phys. Rev. E **65**, 011702 (2002).
[11] M.B. Feller, W. Chen, and Y.R. Shen, Phys. Rev. A **43**, 6778 (1991).
[12] K.R. Makinson and D. Tabor, Proc. R. Soc. London, Ser. A **281**, 49 (1964); C.M. Pooley and D. Tabor, *ibid.* **329**, 251 (1972).
[13] J.C. Wittmann and P. Smith, Nature (London) **352**, 414 (1991).
[14] M. Schott, Synth. Met. **67**, 55 (1994).
[15] Y. Ueda, T. Kuriyama, T. Hari, and M. Ashida, J. Electron Microsc. **43**, 99 (1994).
[16] P. Damman, M. Dosière, M. Brunel, and J.C. Wittmann, J. Am. Chem. Soc. **119**, 4633 (1997).
[17] R. Brownsey and A. Leadbetter, J. Phys. (France) Lett. **42**, 135 (1981).
[18] N.A. Clark, Phys. Rev. Lett. **55**, 292 (1985).
[19] Y. Ouchi, M.B. Feller, T. Moses, and Y.R. Shen, Phys. Rev. Lett. **68**, 3040 (1992).
[20] In fact, it is probable that PI films do not impose a strictly planar orientation of the nematic CCH4, but that the molecules are slightly tilted with respect to the wall plane (pretilt angle), as it has been shown to be the case for mesogenic molecules with cyanobiphenyl head groups.
[21] N.F.A. van der Vegt, F. Müller-Plathe, A. Geleßus, and D. Johannsmann, J. Chem. Phys. **115**, 9935 (2001).
[22] We checked that the nematic alignment is preserved if the PTFE film is covered with an evaporated gold layer of about 500 Å, i.e., when the PTFE chains are isolated from the CCH4 molecules, but the 1D character of the roughness is almost preserved.
[23] A control of the ΔT value within about 0.01 K was obtained previously by applying a tunable pressure onto the sample in a

small, hermetic box maintained at a constant temperature (Clausius-Clapeyron effect). This method was used for studying the growth of CCH4 crystals at undercoolings lower than 0.1 K, see Refs. [6,10]; also see J.C. La Combe, M.B. Koss, L.A. Tennenhouse, E.A. Winsa, and M.E. Glicksman, J. Cryst. Growth **194**, 143 (1998).

[24] S. Akamatsu, G. Faivre, and T. Ihle, Phys. Rev. E **51**, 4751 (1995).

[25] W.K. Burton, N. Cabrera, and F.C. Frank, Philos. Trans. R. Soc. London **243**, 299 (1951).

[26] K.A. Jackson and J.D. Hunt, Trans. Metall. Soc. AIME **236**, 1129 (1966).

[27] W. W. Mullins and R.F. Sekerka, J. Appl. Phys. **35**, 444 (1964).

[28] S. Akamatsu and G. Faivre, Phys. Rev. E **58**, 3302 (1998).

[29] W. Losert, B.Q. Shi, and H.Z. Cummins, Proc. Natl. Acad. Sci. U.S.A. **95**, 431 (1998).

[30] For a review on pattern formation in solidification, see, e. g., M. Cross and P. Hohenberg, Rev. Mod. Phys. **65**, 851 (1993); Also see B. Caroli, C. Caroli, and B. Roulet, in *Solids Far from Equilibrium*, edited by C. Godrèche (Cambridge University Press, Cambridge, 1992).

[31] W.J. Boettinger, S.R. Coriell, A.L. Greer, A. Karma, W. Kurz, M. Rappaz, and R. Trivedi, Acta Mater. **48**, 43 (2000).

[32] D.K. Shangguan and J.D. Hunt, Metall. Trans. A **22A**, 941 (1991).

[33] L.M. Fabietti and R. Trivedi, J. Cryst. Growth **182**, 185 (1997).

[34] P. Kurowski, S. de Cheveigné, G. Faivre, and C. Guthmann, J. Phys. (France) **50**, 3007 (1989).

[35] J.-P. Michel, E. Lacaze, M. Alba, M. Goldman, and F. Rieutord, Surf. Sci. **507–510**, 374 (2002); E. Lacaze (private communication).

[36] D.P. Woodruff, *The Solid-Liquid Interface* (Cambridge University Press, London, 1973); See also, R. Kikuchi and J.W. Cahn, Phys. Rev. B **21**, 1893 (1985).

[37] R.J. Schaefer, M.E. Glicksman, and J.D. Ayers, Philos. Mag. **32**, 725 (1975).

[38] S.R. Coriell and R.F. Sekerka, J. Cryst. Growth **19**, 285 (1973).

[39] S. Bottin-Rousseau, S. Akamatsu, and G. Faivre, Phys. Rev. B **66**, 054102 (2002).